

# A New Efficient Matrix Algorithm for a 3D Component Mode Synthesis (CMS) Model Used on Sound Transmission Problems

M. D. C. Magalhaes<sup>1,2</sup>

**Abstract:** The main goal of this study is to present an alternative and more efficient algorithm for a three-dimensional Component Mode Synthesis model to be used on sound transmission problems. The influence of fluid-structure interaction on airborne sound transmission problems is analysed using this model, which is based on simple volume geometries. In principle, the same procedure can also be applied when the component modes are obtained from alternative numerical techniques. The modal behaviour of acoustic volumes and a partition is implemented in two steps. The novelty of this alternative model is that the structural modes are incorporated on the acoustic CMS components. In other words, each acoustic volume considers not only the acoustic modes of the volumes but also the structural modes of the partition. Comparison is made with predictions based on a modal model of which particle velocity continuity was not incorporated in the formulation.

**Keywords:** Algorithm, component mode synthesis, sound transmission, numerical simulations.

## 1 Introduction

In the literature significant studies have concentrated on analysing sound transmission using uncoupled ‘rigid-walled’ acoustic modes for the acoustic volumes [Magalhaes and Ferguson (2001); Pierce (1981); Fahy (1985)]. In this case the boundary condition at the interface between the acoustic volumes, which is due to the velocity of the partition, cannot be reproduced. The acoustic and the structural response fields are typically expressed in terms of their uncoupled normal modes by means of coupled differential equations for each mode. The structural motion is expressed as a summation over the response of the *in vacuo* natural modes driven

---

<sup>1</sup> Department of Structural Engineering, Federal University of Minas Gerais, Belo Horizonte 31270901, Brazil.

<sup>2</sup> Associate professor, Corresponding author. E-mail: maxdcm@gmail.com

by fluid loading. The acoustic fields in the volumes are determined by a summation of the rigid-walled acoustic modes. According to Fahy (1985), the correct convergence of the modal pressure on the structural interface is obtained due to Gibb's phenomenon, which is an overshoot that occurs whenever basis functions (for instance acoustic mode shapes) are used to represent spatial distributions containing discontinuities, e.g. in the derivatives of the response. In addition, the optimization of algorithms for the solution of particular numerical problems has been widely used by several researchers [Gravvanis, Fidelis-Papadopoulos, Matiskaniadis (2014); Magalhaes (2012); Razzac, Tsotskas, Turek, Kipouros, Savill and Hron (2013); Santos, Matioli and Beck (2012)].

The CMS approach [Craig (1981)] was initially developed and applied to acoustic-structural coupled volumes possessing one-dimensional wave propagation through a limp partition to verify the accuracy and applicability of the approach [Magalhaes and Ferguson (2003)]. Most sound transmission problems require a three-dimensional model for better representation of the sound field distribution. Likewise, the application of the 'limp' mass description is not entirely appropriate in frequency bands higher than the one that includes the fundamental resonance frequency of a partition and so both requirements need to be considered herein. Another development is the extension of the one-dimensional CMS model [Magalhaes and Ferguson (2003)] to the three-dimensional case [Magalhaes and Ferguson (2005)]. This was shown for two simple volume geometries and a rectangular partition. For irregular shapes, the same procedure can be developed when the component modes are obtained from numerical techniques, such as FE, and then applied in the described CMS methodology.

The modal behaviour of acoustic volumes and structural interface was implemented in just one step where a modified version of the three-dimensional model implemented in ref. [Magalhaes and Ferguson (2005)] was considered herein. The partition structural modes were incorporated into the acoustic component formulation as 'acoustic constraint modes'. In other words, the modal description for the structural interface (using normal *in-vacuo* structural modes with the relevant boundary conditions) was incorporated in the source and receiver acoustic components.

The CMS method requires the user to model separate components of a problem in terms of a summation over constraint modes and component normal modes and has previously been applied in structural dynamics. A constraint mode is defined as the static deformation of a subsystem when a unit displacement or velocity is applied to one coordinate of a specific set of 'interface' coordinates. Usually the number of constraint modes considered is equal in number to the number of redundant interface degrees of freedom. The acoustic constraint modes used corresponded to rigid walled conditions on all boundaries other than at the interface with the structure,

which was specified as the actual structural normal modes for these modes. They provide convergence to a better result, so that the particle velocity continuity at the interface can be replicated.

The component normal modes adopted herein were classified according to their boundary conditions as free-interface modes. The acoustic normal modes adopted are taken to be those of the volumes with a flexible wall at the interface and rigid walls on all other boundaries. The number of normal modes chosen depends upon the frequency range of the calculations and convergence requirements.

In summary, the aim of this paper is to develop an alternative CMS model that incorporates interface particle velocity continuity in the formulation for the prediction of noise transmission between two volumes. The Component Mode Synthesis (CMS) method [Craig (1981)] was used for the development of this alternative model which is based on the one developed previously [Magalhaes and Ferguson (2005)]. Subsequently, the CMS model implemented was then compared with the traditional modal model [Fahy (1985)].

## **2 Sound transmission mechanism– Theoretical background**

The mechanism of sound transmission may be considered in terms of the radiated sound field from an elastic partition, itself excited by a sound field in a source room. The partition, modelled by a thin plate, has a response to acoustic excitation, which consists of both free and forced bending waves. Freely travelling bending waves are generated when the plate is excited at its natural frequencies. As a result of the plate edges, these waves interact with each other producing the plate mode of vibration. On the other hand, forced waves occur due to pressure fluctuations which force the plate to move in such a way that free-bending waves are not significantly generated. The spatial distribution of the forcing produces a response that is similar in its spatial response.

In terms of radiation efficiency, which is a non-dimensional measure of the sound power radiated by a vibrating surface into an adjacent fluid [Fahy (1985)], the generation of free bending waves is more important at frequencies above the critical frequency of the panel, where the natural modes of the partition consist of wave motion with phase velocity greater than the speed of sound travelling in air. In this condition, sound power is radiated efficiently [Fahy (1985)]. Below the critical frequency, the free waves are produced but are not significant for sound transmission. Forced waves at the acoustic wave number are predominant when a panel vibrates at frequencies lower than its critical frequency. They are common when a panel is excited acoustically [Fahy (1985)]. In addition, when a sound wave is incident upon a partition, the response, which is frequency dependent, is also dependent on

the radiation impedance of the modes of the partition. Thus, the air or fluid on the receiver side of the plate is excited, and sound waves propagate away from the plate into the receiving volume.

Below the first panel resonance, there is an increase in SRI with decreasing frequency. In this frequency range, the panel moves with the pressure fluctuation to transmit sound and has a very small frequency response. The vibration can be reduced by stiffening the panel hence causing an increase in the SRI.

### ***2.1 Sound transmission through an infinite partition***

In general, the sound transmission theory for uniform and unbounded panels has widely been used to approximate the sound transmission loss of a bounded panel in a baffle. Of course, some assumptions, such as the random-incidence field over the partition, as well as a limited frequency range (in which the acoustical wavelength is smaller than the plate size), have been considered. For instance, the normal incidence Mass Law theory is basically derived from an idealized model of normal incidence transmission through an unbounded partition [Pierce (1981)]. On the other hand, the diffuse field transmission coefficient can be obtained by considering the whole range of incident angles with equal likelihood. In room acoustics there is an important parameter, namely the ‘Schroeder’ frequency [Fahy (2000)], at which the frequency or modal overlap of the room modes is large enough for the sound field to be considered diffuse.

Two measures of the effectiveness of a partition in reducing sound transmission are the transmission efficiency and the Sound Reduction Index. A transmission efficiency parameter  $\tau$  is defined as the ratio of transmitted to incident acoustic power. A positive value of the Sound Reduction Index corresponds to a reduction of the transmitted power compared to the incident. The mass law SRI expressions for normal ( $SRI_n$ ), field ( $SRI_f$ ) and diffuse ( $SRI_d$ ) incidence are given in Fahy (2000).

### ***2.2 Sound transmission through a finite partition in a baffle***

A finite-size and baffled rectangular plate is a more realistic model than the infinite one described previously. The transmission is characterized by boundary effects, which lead to the formation of standing-wave modes and resonance. Leppington [Leppington, Broadbent and Heron (1989)] proposed a different formula for the transmission efficiency  $\tau_{Lep}$  averaged over all incidence angles and over a frequency band. The resonant  $\tau_{res}$  and non-resonant contributions  $\tau_{nr}$  are expressed in [Leppington, Broadbent and Heron (1989)].

The resonant contribution  $\tau_{res}$  is due to the modes excited at or near resonance,

which produce a large partition deflection but are inefficient in terms of sound power radiation. The non-resonant contribution  $\tau_{nr}$  corresponds to that from the small amplitude off-resonant modes. However, for these non-resonant modes sound energy is radiated efficiently and their wavenumbers are smaller than the acoustic wavenumber. According to Leppington [Leppington, Broadbent and Heron (1989)], there is good agreement between the transmission values obtained via solely the non-resonant contribution  $\tau_{nr}$  and experimental tests with no need for an *ad hoc* correction. As mentioned previously, it is assumed that the plate is simply-supported. It is also assumed that the transmission efficiencies represent an average over a large number of modes and over all incidence angles.

### 3 The CMS Method for the 3D case – Matrix formulation

As in the three dimensional case developed in ref. [Magalhaes and Ferguson (2005)], the implementation of the modified CMS method for the 3D case was also based on the selection of the sets of modes, definition of the constraint equations and system synthesis. Two rigid-walled rectangular cross section volumes with a common elastic partition at the interface, as shown in figure 1, are considered as only two distinct CMS components, instead of three CMS components defined in ref. [Magalhaes and Ferguson (2005)]. The first consists of the acoustic fluid volume, being defined for  $x = -L_{x1}$  to  $x = 0$ . The second component is the receiving acoustic fluid volume, which is defined as varying from  $x = 0$  to  $x = L_{x2}$ . Both components have been considered with the same cross-section, but the extension to other volumes is also straight forward. The elastic simply-supported partition, which separates the two volumes, is represented dynamically by constraint flexural modes included on both CMS acoustic components. A harmonic constant amplitude volume velocity source is placed in one corner of the source volume, so that all acoustic modes can be excited. It is assumed that the fluid velocity function  $\dot{\epsilon}(x, y, z, t)$  can be written in terms of the generalized velocity potential  $\bar{\Phi}$  (scalar quantity) by the modal transformation [Fahy (1985)]

$$\dot{\epsilon} = \left( \Psi_x \vec{i} + \Psi_y \vec{j} + \Psi_z \vec{k} \right) \bar{\Phi} \quad (1)$$

where  $\Psi_x$ ,  $\Psi_y$  and  $\Psi_z$  are matrices which consist of pre-selected normal velocity modes for a rigid walled volume plus constraint modes, representing the fluid velocity distribution in the  $x$ ,  $y$  and  $z$  directions respectively; The fluid velocity function and the generalized velocity potential are defined as  $\dot{\epsilon}(x, y, z, t) = \frac{\partial \epsilon(x, y, z, t)}{\partial t}$  and  $\dot{\epsilon} = (\dot{u}, \dot{v}, \dot{w}) = \nabla(\Phi)$  respectively.

The modal matrices for the source component are given by

$$\Psi_{x1} = s_{x1} \left[ \Psi_{n1} \quad \Psi_{c1} \right] \quad (2)$$

$$\Psi_{y1} = s_{y1} \left[ \Psi_{l_1} \quad \Psi_{c_1} \right] \tag{3}$$

$$\Psi_{z1} = s_{z1} \left[ \Psi_{q_1} \quad \Psi_{c_1} \right] \tag{4}$$

where the subscript  $c_1$  represents the constraint mode number. The subscripts  $n$ ,  $l$ , and  $q$  denote the normal mode number of a particular mode in the  $x$ ,  $y$  and  $z$  directions respectively.  $s_{x1}$ ,  $s_{y1}$  and  $s_{z1}$  represent scale constants whose units are such that  $\Psi_{x1}$ ,  $\Psi_{y1}$  and  $\Psi_{z1}$  have dimensions of  $(\text{mass})^{-0.5}$ . The matrix  $\Psi_{x1}$  consists of a set of fixed-fixed interface normal modes ( $\Psi_{n_1}$ ) plus a set of fixed-*structural* constraint modes ( $\Psi_{c_1}$ ) in the  $x$  direction. Likewise, the matrix  $\Psi_{y1}$  is comprised of a set of fixed-fixed interface modes ( $\Psi_{l_1}$ ) in the  $y$  direction plus the set of fixed-*structural* modes ( $\Psi_{c_1}$ ), which is due to the contribution of the constraint modes to the fluid particle velocity in the  $x$  normal direction. Finally, matrix  $\Psi_{z1}$  consists of a set of fixed-fixed interface normal modes ( $\Psi_{q_1}$ ) plus the set of modes  $\Psi_{c_1}$ .

The set of constraint modes  $\Psi_{c_1}$  contributes to the fluid particle velocity distribution only in the  $x$  direction, considering that the partition normal velocity equals the fluid particle velocity at the interface. This is justified by the fact that the interface between components is only in the constant plane  $x=0$ . The selected orthogonal and constraint modes were defined as shape functions satisfying the geometric boundary conditions for each acoustic component. By application of the well-known relationship between velocity potential and particle velocity [Fahy, (1985)], the orthogonal modes  $\Psi_{n_1}$  (in the  $x$  direction) and their contributions to the fluid particle velocity in the  $y$  and  $z$  directions ( $\Psi_{l_1}$  and  $\Psi_{q_1}$ ) can be expressed by [Magalhaes and Ferguson (2005)]

$$\Psi_{n_1}(x,y,z,t) = -k_{n_1} \sin(k_{n_1}x) \cos(k_{l_1}y) \cos(k_{q_1}z) \quad \text{for} \quad -L_{x1} \leq x \leq 0 \tag{5}$$

$$\Psi_{l_1}(x,y,z,t) = -k_{l_1} \cos(k_{n_1}x) \sin(k_{l_1}y) \cos(k_{q_1}z) \quad \text{for} \quad 0 \leq y \leq L_{y1} \tag{6}$$

$$\Psi_{q_1}(x,y,z,t) = -k_{q_1} \cos(k_{n_1}x) \cos(k_{l_1}y) \sin(k_{q_1}z) \quad \text{for} \quad 0 \leq z \leq L_{z1} \tag{7}$$

where  $k_{n_1}$ ,  $k_{l_1}$  and  $k_{q_1}$  are equal to  $n_1\pi / (L_{x1})$ ,  $l_1\pi / L_{y1}$  and  $q_1\pi / L_{z1}$  respectively. It is seen that the natural modes given by eqs. (5), (6) and (7) have units equal to  $[\text{m}^{-1}]$ .

As mentioned previously, an additional set of constraint modes  $\Psi_{c_1}$ , which satisfies zero velocity on  $x = -L_{x1}$  and the structure velocity modal distribution in the  $x$  direction on  $x = 0$  over the partition area is used for the source room. In principle, the elastic partition covers the whole of the common boundary ( $x = 0$ ). For the source room component, the constraint modes  $\Psi_{c_1}$  (in the  $x$  direction) are then given by

$$\Psi_{c_1}(x,y,z,t) = \left( 1 + \frac{x}{L_{x1}} \right) \phi_{p,q}(y,z) \tag{8}$$

where  $\phi_{p,q}(y,z)$  is the analytical mode shape for a simply-supported rectangular plate *in vacuo*. It is given by

$$\phi_{p,q}(y,z) = \sin(k_{py}y) \sin(k_{qz}z) \quad (9)$$

where  $k_{py} = p\pi/L_{y_p}$  and  $k_{qz} = q\pi/L_{z_p}$  are the plate modal wavenumbers in the  $y$  and  $z$  directions respectively. For general boundary conditions, the structure mode shape can be obtained numerically, for instance via the FEM.

Eqs. 8 and 9 apply over the area of the partition, even if it might only cover a partial area of the whole interface (common wall). It is seen that this set of Eqs. (8-9) do not have the same dimensions of those equations defined previously in Eqs. (5-7).

However, all original mode shape vectors defined above, the natural and constraint modes, were normalized to the more useful mass-normalized mode shape vectors [Craig (1981)]. It should be noted that the natural modes have units equal to  $[m^{-1}]$  and the constraint modes are dimensionless, while after normalization [Craig (1981)], the mass-normalized vectors defined in Eqs. (2-4) have dimensions of  $(\text{mass})^{-0.5}$ .

A linear function was chosen to represent the particle velocity distribution in the  $x$  direction, as higher order functions did not provide better convergence. The particle velocity of a fluid is defined by the first order derivative of its velocity potential. A certain function appears in eq. (9), which represents the *constraint* modes velocity contributions in the  $y$  and  $z$  directions respectively.

Additionally, it is assumed that the set of normal structural modes  $\phi_p$  are the flexural vibration mode shapes of a simply supported isotropic rectangular thin plate [Craig (1981)]. No constraint modes are necessary for the structural component and other structural boundary conditions could similarly be considered.

The modal matrices for the receiving component can be expressed as

$$\Psi_{x2} = s_{x2} \begin{bmatrix} \Psi_{n2} & \Psi_{c2} \end{bmatrix} \quad (10)$$

$$\Psi_{y2} = s_{y2} \begin{bmatrix} \Psi_{l2} & \Psi_{c2} \end{bmatrix} \quad (11)$$

$$\Psi_{z2} = s_{z2} \begin{bmatrix} \Psi_{q2} & \Psi_{c2} \end{bmatrix} \quad (12)$$

Likewise for the source component,  $s_{x2}$ ,  $s_{y2}$  and  $s_{z2}$  represent scale constants whose units are such that  $\Psi_{x2}$ ,  $\Psi_{y2}$  and  $\Psi_{z2}$  have dimensions of  $(\text{mass})^{-0.5}$ . The matrix  $\Psi_{x2}$  comprises of a set of fixed-fixed interface normal modes ( $\Psi_{n2}$ ) plus a set of free-fixed constraint modes ( $\Psi_{c2}$ ) in the  $x$  direction. The matrix  $\Psi_{y2}$  is composed of a set of fixed-fixed interface normal modes ( $\Psi_{l2}$ ) plus another set of free-fixed modes ( $\Psi_{c2}$ ) in the  $x$  direction, which is due to the contribution of the constraint modes  $\Psi_{c2}$  to the fluid particle normal velocity. In the same way, matrix  $\Psi_{z2}$  comprises

a set of fixed-fixed interface normal modes ( $\Psi_{q_2}$ ) plus the set of constraint modes. As for the source room, the set of free-fixed constraint modes  $\Psi_{c_2}$  is sufficient for the formulation of the problem.

Additionally, the (x,y,z) particle velocity Cartesian components for the receiving volume are given respectively by

$$\Psi_{n_2}(x, y, z, t) = -k_{n_2} \sin(k_{n_2}x) \cos(k_{l_2}y) \cos(k_{q_2}z) \quad \text{for } 0 \leq x \leq L_{x_2} \quad (13)$$

$$\Psi_{l_2}(x, y, z, t) = -k_{l_2} \cos(k_{n_2}x) \sin(k_{l_2}y) \cos(k_{q_2}z) \quad \text{for } 0 \leq y \leq L_{y_2} \quad (14)$$

$$\Psi_{q_2}(x, y, z, t) = -k_{q_2} \cos(k_{n_2}x) \cos(k_{l_2}y) \sin(k_{q_2}z) \quad \text{for } 0 \leq z \leq L_{z_2} \quad (15)$$

where  $k_{n_2}$ ,  $k_{l_2}$  and  $k_{q_2}$  are equal to  $n_2\pi/L_{x_2}$ ,  $l_2\pi/L_{y_2}$  and  $q_2\pi/L_{z_2}$  respectively.

The constraint modes  $c_2$  in the x direction have velocity components then given by

$$\Psi_{c_2}(x, y, z, t) = \left(1 + \frac{x}{L_{x_2}}\right) \phi_{p,q}(y, z) \quad (16)$$

where  $\phi_{p,q}(y, z)$  was defined previously.

It is also seen that for the receiving component the constraint modes given by Eq. (16) are dimensionless while the natural modes defined by Eqs. (13), (14) and (15) have units [1/m].

Although the fluid particle velocity was considered in all directions (see Eq. (1)), for calculating the dynamic response of the acoustic components 1 and 2 the compatibility equations describing velocity continuity were only formulated in terms for the x direction normal to the partition or interface. Hence although the fluid velocity function is equal to  $\dot{\epsilon} = (\dot{\epsilon}_x, \dot{\epsilon}_y, \dot{\epsilon}_z)$ , one only needs  $\dot{\epsilon}_x$  for the formulation of the constraint equations at the interface. On this alternative formulation, the structural partition was not considered as an extra modal system. Thus, sufficient compatibility or constraint function is given by

$$C = \int_S \left( \left( \frac{\partial \epsilon_{x,1}}{\partial t} \right) \Big|_{x=0} - \left( \frac{\partial \epsilon_{x,2}}{\partial t} \right) \Big|_{x=0} \right)^2 dS = \int_S \left( (\dot{\epsilon}_{x,1})|_{x=0} - (\dot{\epsilon}_{x,2})|_{x=0} \right)^2 dS \quad (17)$$

where  $\epsilon_{x,1}$  and  $\epsilon_{x,2}$  are the fluid particle displacements in the x direction for volumes 1 and 2 respectively and S is the surface area of the interface.

This equation is used to determine a reduced set of generalized coordinates equal to the difference between the number of component coordinates and the number of constraint conditions. In situations where a partition covers only a part of the common boundary the integral in the constraint equation is evaluated only over the partition area.

It is implicit in eq. (17) that the same reference coordinate is used for all components. It is not a linear problem in the generalised co-ordinates to set the constraint function  $C_1$  to zero, instead one tries to minimise the error in a least squares sense by minimizing the function. Hence, the following matrix form for the constraint equations can be obtained

$$\frac{\partial C}{\partial \dot{\epsilon}_{x,1}} = \frac{\partial C}{\partial \dot{\epsilon}_{x,2}} = 0 \quad (18)$$

$$\text{or } \mathbf{R}_c \bar{\mathbf{G}} = 0 \quad (19)$$

$$\text{where } \bar{\mathbf{G}} = [ \bar{\Phi}_{c1} \quad \bar{\Phi}_{c2} ]^T \quad \text{and } \mathbf{R}_c = [ \mathbf{R}_1; \mathbf{R}_2 ] \quad (20)$$

$$\text{and } \mathbf{R}_1 = \begin{bmatrix} 0 & R_{11} \\ 0 & R_{12} \end{bmatrix} \quad \mathbf{R}_2 = \begin{bmatrix} 0 & R_{21} \\ 0 & R_{22} \end{bmatrix} \quad (21)$$

The column vector  $\bar{\mathbf{G}}$  and the matrix  $\mathbf{R}_c$  contain the system generalized coordinates and the geometrical coupling coefficients respectively.

The sub-matrices  $R_{11}$ ,  $R_{12}$ ,  $R_{21}$  and  $R_{22}$  defining the geometrical coupling are given by

$$R_{11} = \int_S (\Psi_{c1})^T (\Psi_{c1}) dS \quad (22)$$

$$R_{12} = \int_S (\Psi_{c1})^T (\Psi_{c2}) dS \quad (23)$$

$$R_{21} = \int_S (\Psi_{c2})^T (\Psi_{c1}) dS \quad (24)$$

$$R_{22} = \int_S (\Psi_{c2})^T (\Psi_{c2}) dS \quad (25)$$

The acoustic modal matrices  $\Psi_{x1}$  and  $\Psi_{x2}$  are defined in eqs. (2) and (10) respectively. No terms exist in coupling between the normal modes of the volumes ( $\Psi_{n1}$  or  $\Psi_{n2}$ ) and the constraint modes ( $\Psi_c$ ), as the former have zero velocity at the interface ( $x = 0$ ). The matrix  $R_{12}$  and  $R_{21}$  are also diagonal matrices due to orthogonality of the structural modes.

In this section the dynamic properties of an acoustic component driven by a volume velocity source are derived using the direct application of Lagrange's equations [Craig (1981)]. It is necessary to formulate the scalar potential and kinetic energy

quantities. The kinetic energy  $T_A$  for an acoustic volume  $V_1$  can be expressed as [Pierce (1981)]

$$T_A = \frac{1}{2} \rho_o \int_{V_1} ((\dot{\epsilon})^*)^T (\dot{\epsilon}) dV \tag{26}$$

Substituting eq. (1) into eq. (26), the expression for the total kinetic energy using all of the modes employed in the formulation then becomes

$$T_A = \frac{1}{2} (\bar{\Phi}^T)^* \rho_o \left\{ \int_{V_1} ((\Psi_x)^T \Psi_x) dV_1 + \int_{V_1} ((\Psi_y)^T \Psi_y) dV_1 + \int_{V_1} ((\Psi_z)^T \Psi_z) dV \right\} (\bar{\Phi}) \tag{27}$$

The potential energy of a fluid inside a volume  $V_1$  is defined in terms of a velocity potential function  $\Phi$  as [Pierce (1981)]

$$V_A = \frac{1}{2} \int_{V_1} \left( \kappa \rho_o^2 \frac{\partial(\Phi^T)^*}{\partial t} \frac{\partial\Phi}{\partial t} \right) dV_1 \tag{28}$$

where  $\kappa = \frac{1}{\rho_o c_o^2}$  is the compressibility of the fluid (29)

Using the relationship between sound pressure and velocity potential, the potential energy can then be expressed in terms of pressure as

$$V_A = \frac{1}{2} \int_{V_1} \left( \kappa (p^*)^T p \right) dV_1 \tag{30}$$

Assuming that the acoustic disturbances in each component are sufficiently small, a linear relationship between pressure and the fluid velocity  $\dot{\epsilon}(x,y,z,t)$  can be written as<sup>2</sup>

$$p = \frac{1}{j\omega\kappa} \text{div}(\dot{\epsilon}) \tag{31}$$

and  $\text{div}(\dot{\epsilon}) = \nabla \cdot \dot{\epsilon} = \left( \frac{\partial\Psi_x}{\partial x} + \frac{\partial\Psi_y}{\partial y} + \frac{\partial\Psi_z}{\partial z} \right) \bar{\Phi}$  (32)

where  $\kappa$  is defined in eq. (29) and  $\bar{\Phi}$  is the velocity potential of the fluid.

Substituting eq. (31) and (32) into eq. (30), the expression for potential energy becomes

$$V_A = \frac{1}{2\kappa} (\bar{\Phi}^T)^* \left\{ \int_{V_1} \left( \frac{\partial(\Psi_x)^T}{\partial x} \frac{\partial \Psi_x}{\partial x} \right) dV_1 + \int_{V_1} \left( \frac{\partial(\Psi_y)^T}{\partial y} \frac{\partial \Psi_y}{\partial y} \right) dV_1 + \int_{V_1} \left( \frac{\partial(\Psi_z)^T}{\partial z} \frac{\partial \Psi_z}{\partial z} \right) dV_1 \right\} (\bar{\Phi}) \quad (33)$$

For non-conservative systems, a dissipation function [Ghlaim and Martin (1986); Klein and Dowell (1974)] must be included. For an acoustic component, it can be expressed as

$$D = \frac{1}{2} (\bar{\Phi}^T)^* \rho_o \left\{ \int_{V_1} ((\Psi_x)^T 2 \omega_N \zeta_N \Psi_x) dV_1 + \int_{V_1} ((\Psi_y)^T 2 \omega_N \zeta_N \Psi_y) dV_1 + \int_{V_1} ((\Psi_z)^T 2 \omega_N \zeta_N \Psi_z) dV_1 \right\} \bar{\Phi} \quad (34)$$

where  $\zeta_N$  is the viscous modal damping ratio matrix for the components and  $\omega_N$  is the modal matrix of natural frequencies. The damping matrix can then be derived from the above expression. Linear viscous damping was adopted for the purpose of simplification, as this is a reasonable choice for highly reverberant acoustic spaces [Fahy (1985)].

The system equations of motion can be obtained for a damped system by using Lagrange's equation of motion [Craig (1981)] as follows

$$\frac{\partial}{\partial t} \left( \frac{\partial L}{\partial \dot{q}_i} \right) - \frac{\partial L}{\partial q_i} + \frac{\partial D}{\partial \dot{q}_i} = Q_i \quad i = 1, 2, \dots, n \quad (35)$$

where  $L$  is the Lagrangian for the system of coupled components described below,  $D$  is the damping dissipation function and  $q_i$  are the elements of the generalized coordinate  $\bar{\Phi}$ . In addition, it is assumed that the modes are real.  $Q_i$  is the time-dependent generalized volume velocity source strength in the case of a source within an acoustic volume or generalized force for a general system. The Lagrangian is defined by [Craig (1981)]

$$L = T_A - V_A + \lambda^T \mathbf{R}_c \bar{G} \quad (36)$$

where  $\lambda$  is a Lagrange multiplier vector which enforces interface compatibility. It has the dimension of force.

The dynamic properties of a separate acoustic component 1 may be determined via Lagrange’s equations (Eq. 35), which lead to the following equations of motion

$$M_1^{3D} \ddot{\Phi}_1 + C_1^{3D} \dot{\Phi}_1 + K_1^{3D} \Phi_1 - (R_1)^T \lambda_1 = Q_1^{3D} \tag{37}$$

where

$$M_1^{3D} = \rho_o \left\{ \int_{V_1} ((\Psi_{x1})^T \Psi_{x1}) dV_1 + \int_{V_1} ((\Psi_{y1})^T \Psi_{y1}) dV_1 + \int_{V_1} ((\Psi_{z1})^T \Psi_{z1}) dV_1 \right\} \tag{38}$$

$$K_1^{3D} = \rho_o c^2 \int_{V_1} \left( \frac{\partial(\Psi_{x1})^T}{\partial x} \frac{\partial \Psi_{x1}}{\partial x} \right) dV_1 + \int_{V_1} \left( \frac{\partial(\Psi_{y1})^T}{\partial y} \frac{\partial \Psi_{y1}}{\partial y} \right) dV_1 + \int_{V_1} \left( \frac{\partial(\Psi_{z1})^T}{\partial z} \frac{\partial \Psi_{z1}}{\partial z} \right) dV_1 \tag{39}$$

$$C_1^{3D} = 2\omega_{NP} \left\{ \int_{V_1} ((\Psi_{x1})^T \zeta_N \Psi_{x1}) dV_1 + \int_{V_1} ((\Psi_{y1})^T \zeta_N \Psi_{y1}) dV_1 + \int_{V_1} ((\Psi_{z1})^T \zeta_N \Psi_{z1}) dV_1 \right\} \tag{40}$$

$$Q_1^{3D} = j\omega\rho_o Q_o \int_{\Psi_{x1}} \delta_o(x - x_o, y - y_o, z - z_o) dx \tag{41}$$

$\delta_o(x - x_o, y - y_o, z - z_o)$  is the three-dimensional Dirac delta function representing a point volume velocity source at  $(x_o, y_o, z_o)$ , and  $M_1^{3D}$ ,  $K_1^{3D}$ , and  $C_1^{3D}$  are scalar quantities representing the modal mass, stiffness and damping matrices for the fluid volume respectively.  $Q_1^{3D}$  is the column matrix of generalized volume velocity source strength where the individual terms relate to the excitation of individual model components.  $R_1$  is the matrix defined in eq. (21).  $\lambda_1$  is a column vector with a number of rows equal to the total number of constraint modes in component 1 and the total number of constraint modes in component 2.

As a consequence of classifying the modes into two categories, namely constraint modes and normal modes, the mass, stiffness and damping matrices are partitioned into sub-matrices as follows [Magalhaes and Ferguson (2005)]

$$M_1^{3D} = \begin{bmatrix} m_{NN} & m_{NC} \\ m_{NC}^T & m_{CC} \end{bmatrix}; \quad K_1^{3D} = \begin{bmatrix} k_{NN} & k_{NC} \\ k_{NC}^T & k_{CC} \end{bmatrix}; \quad C_1^{3D} = \begin{bmatrix} c_{NN} & c_{NC} \\ c_{NC}^T & c_{CC} \end{bmatrix}; \tag{42}$$

The sub-matrix  $m_{NN}$ ,  $k_{NN}$  and  $c_{NN}$  are diagonal matrices. This is true due to the orthogonality property of these component modes. The order of these matrices depends upon the number of modes chosen for the analysis. The sub-matrices  $m_{CC}$ ,  $k_{CC}$  and  $c_{CC}$  are square matrices associated with the constraint modes; their orders are equal to the number of constraints. Finally, the rectangular matrices  $m_{NC}$ ,  $k_{NC}$  and  $c_{NC}$  are associated with the coupling between the normal and constraint modes, as these are generally not orthogonal and cross-terms exist in the potential and kinetic energy expressions as well as in the dissipation function.

The equations of motion for the source volume (acoustic component 1) and the receiving volume (acoustic component 2) are expressed in terms of their generalized coordinates  $\bar{\Phi}$  as

$$M_1^{3D} \ddot{\bar{\Phi}}_1 + C_1^{3D} \dot{\bar{\Phi}}_1 + K_1^{3D} \bar{\Phi}_1 - R_1^T \lambda_1 = Q_1^{3D} \quad (43)$$

$$M_2^{3D} \ddot{\bar{\Phi}}_2 + C_2^{3D} \dot{\bar{\Phi}}_2 + K_2^{3D} \bar{\Phi}_2 - R_2^T \lambda_2 = 0 \quad (44)$$

where  $\lambda_1$  and  $\lambda_2$  are column vectors of Lagrange multipliers for components 1 and 2 respectively. The set of equations presented above as well as the dynamic properties of the acoustic components  $M^{3D}$ ,  $C^{3D}$ , and  $K^{3D}$  and the generalized volume velocity source strength  $Q^{3D}$  can all be derived as shown previously using Lagrange's equations of motion.

The coupled set of equations for the entire system is then given by

$$\mu \ddot{\bar{G}} + \zeta \dot{\bar{G}} + \chi \bar{G} - \lambda R_c = Q_s \quad (45)$$

$$\text{and } R_c \bar{G} = 0 \quad (46)$$

where

$$\lambda = \begin{Bmatrix} \lambda_1 \\ \lambda_2 \end{Bmatrix}; \quad \mu = \begin{bmatrix} M_1^{3D} & 0 \\ 0 & M_2^{3D} \end{bmatrix}; \quad \zeta = \begin{bmatrix} C_1^{3D} & 0 \\ 0 & C_2^{3D} \end{bmatrix}; \quad \chi = \begin{bmatrix} K_1^{3D} & 0 \\ 0 & K_2^{3D} \end{bmatrix};$$

and  $Q_s = [ Q_1^{3D} \quad 0 ]^T$ . The matrices  $\mu$ ,  $\zeta$  and  $\chi$  are the modal mass, damping and stiffness matrices respectively.  $Q_s$  is a column vector containing the generalized 'forces' exerted on the components. It can also be shown that the coordinates  $\bar{G}$  are not linearly independent in the set of Eqs. (45), due to the constraint equations (Eqs. 46).

The matrix of generalized coordinates  $\bar{G}$  cannot easily be rearranged and partitioned into dependent and linearly independent coordinates as in the one-dimensional case [Magalhaes and Ferguson (2003)].

Alternatively, eqs. (45) and (46) may be written in the partitioned form [Klein and Dowell (1974)]

$$\begin{bmatrix} (\chi - \omega^2\mu + j\omega\zeta) & -R_c \\ R_c^T & 0 \end{bmatrix} \begin{Bmatrix} \bar{G} \\ \lambda \end{Bmatrix} = \begin{Bmatrix} Q_s \\ 0 \end{Bmatrix} \quad (47)$$

The use of the Lagrange's Multiplier technique for the present situation, whilst more tedious than the transformation matrix technique, permits the incorporation of the constraint equations in a systematic manner. Eq. (47) can be solved numerically by the application of a pseudo-inversion technique, e.g. using Singular Value Decomposition [Gialamas, Tsahalis, Otte, Van Der Auwaraer and Manolas (2001)]. One decision that has to be made by the analyst who uses component modes is how many modes to use. In order to prevent the matrices becoming singular, the number of constraint modes should be equal in number to the number of redundant constraints. In this case, the set of equations in (47) is overdetermined.

#### 4 Results and discussion

All numerical simulations and results are presented for the three dimensional problem, which also includes the modal contribution of the partition.

##### 4.1 Comparison between the 3D Modified CMS and the Modal approach

First, a comparison between the CMS and the modal model is presented using a particular numerical model. A flexible partition with dimensions equal to 1m x 1.2m was considered over the whole common interface. The source and receiving volume dimensions were equal to 2.5m x 1.0m x 1.2m (depth by height by width). A constant viscous modal damping equal to  $\zeta = 0.005$  was used for both the normal and constraint modes. Figure 1 shows that a monopole source with constant volume velocity equal to  $3 \times 10^{-5} \text{ m}^3/\text{s}$  was placed at one corner of the source volume (-2.5,0,0).

A modal model was used to calculate a reference solution to compare with the one obtained using the CMS model. The analytical Modal model developed and implemented here is an extension of the set of integro-differential equations presented in ref. [Fahy (1985)] to a system comprising two coupled rooms and a simply supported partition. Thus, the problem involving sound transmission between two connected rooms can be tackled. For the Modal model, the acoustic and the structural response fields are expressed in terms of their uncoupled normal modes by means of differential equations for each mode. Therefore, the structural motion is expressed as a summation over the response of the *in vacuo* natural modes driven by fluid loading. The acoustic field of rigid-walled rectangular components has

been determined by the summation of the acoustic modes over the fluid volume. In fact, these acoustic modes in the source room were excited by a generalized volume velocity source. According to Fahy (1985), the correct convergence of the modal pressure on the partition surface is obtained due to the Gibb's phenomenon, which is an overshoot that occurs whenever basis functions (for instance acoustic mode shapes) are used to represent spatial distributions containing discontinuity of slope. The effect of the inclusion of the 0 Hz bulk elastic mode in the Modal model has been checked by eliminating it from the calculations (not shown). As a result, the variation of sound pressure in the source and receiving volumes for the CMS model tended to zero at frequencies below their first 'dynamic' modes.

Table 1 shows two groups of natural frequencies of rooms, obtained analytically, using the modal and the modified 3D CMS models.

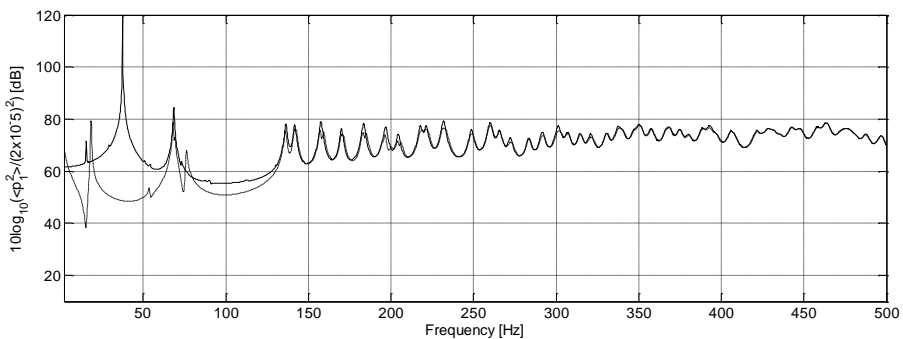
In Fig. 1 peaks at about 136 Hz and 141 Hz can be seen in the response of both the source and receiving volumes. However, there are some extra peaks in the response for the receiving volume, which correspond to coupled modes of the complete system. This is because the receiving volume controlled modes are weakly excited by the source volume.

Table 1: Comparison between groups of natural frequencies of the rooms obtained analytically using both modal and Modified CMS models.

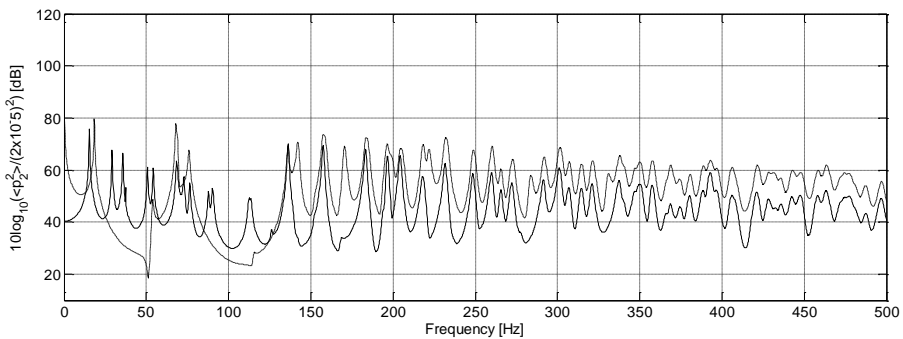
Mode Number	Uncoupled $F_N$ (Hz) (Modal model)	Uncoupled $F_N$ (Hz) (Modified 3D CMS model)
1	0	0
2	68.0	68.5
3	136.0	136.3
4	141.7	141.6
5	157.1	157.5
6	170.0	170.1
7	183.1	185.0
8	196.4	196.8
9	204.0	204.3
10	217.7	218.1

Figs. 2 and 3 show the Noise Reduction (NR) values in narrow and 1/3 octave bands respectively. The difference in the NR between the CMS and Modal models in 1/3 octave bands tends to be less than about 15 dB (for both materials considered herein) at centre frequencies greater than 150 Hz. Below 150 Hz, the results

show poor agreement. In Fig. 3 an alternative comparison shows that there is a fair agreement between the CMS model and Leppington’s approach [Leppington, Broadbent and Heron (1989)] for the lighter material. The calculated ‘Schroeder’ frequency [Pierce (1981)] was 1,115 Hz for the source and receiving rooms. They were greater than the highest 1/3 octave band centre frequency considered in the model configuration. Thus, the predicted system response was strongly influenced by individual modes of the rooms. The NR results obtained using the models may not be appropriate, for the acoustic fields involved are not diffuse.



(a)



(b)

Figure 1: Comparison between the CMS and a Modal model in terms of spatial-average mean square sound pressure (in narrow bands). The panel mass per unit area is equal to  $\rho h = 8.06 \text{ kg/m}^2$  and  $E = 2.12 \times 10^9 \text{ N/m}^2$ . (a) source:  $10 \log_{10} (\langle \bar{p}_1^2 \rangle / p_o^2)$  [dB re  $2 \times 10^{-5} \text{ Pa}$ ]; (b) receiver:  $10 \log_{10} (\langle \bar{p}_2^2 \rangle / p_o^2)$  [dB re  $2 \times 10^{-5} \text{ Pa}$ ]. The subscript 1 and 2 indicates source and receiving volumes respectively; — CMS model; - - - Modal model.

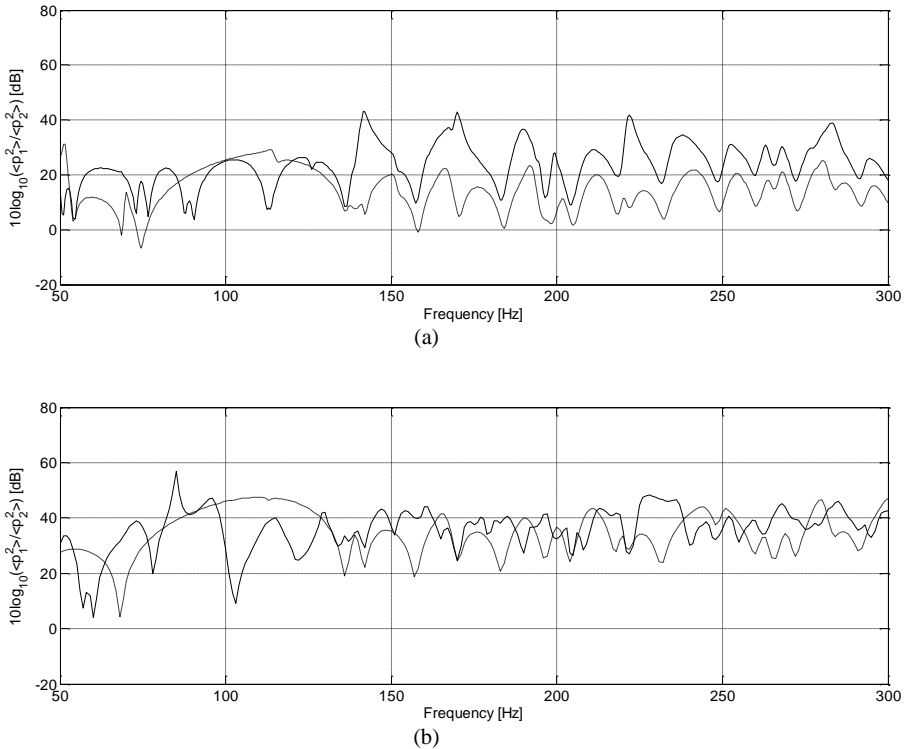


Figure 2: The variation of the Noise Reduction ( $\text{NR} = 10 \log_{10} (\langle \bar{p}_1^2 \rangle / \langle \bar{p}_2^2 \rangle)$ ) [dB re 1] in narrow bands normalized to the system power input. (a). The panel mass per unit area is equal to  $\rho h = 8.06 \text{ kg/m}^2$  and  $E = 2.12 \times 10^9 \text{ N/m}^2$ . (b) The panel mass per unit area is equal to  $\rho h = 78.50 \text{ kg/m}^2$  and  $E = 210 \times 10^9 \text{ N/m}^2$ . The subscript 1 and 2 indicates source and receiving volumes respectively; — CMS model; - - - Modal model.

In addition, Fig. 3 shows that significant differences between the models occur at low frequencies. As the frequency increases, a fairly good agreement is obtained between the models. Moreover, the CMS result shows fairly good agreement with those obtained via Leppington's approach and with the field incidence Mass Law. For the model considered the incidence Mass Law appears to still be underestimating the NR at the higher frequencies being considered here. The spatial results are presented in terms of normalized mean square pressure and particle velocity distribution at 190 Hz over a certain position (plane) that has been specified *a priori*. This particular frequency, which do not necessarily coincide with the fundamental room modes, was arbitrarily chosen above the lowest natural frequency of the receiving room, above which tangential and oblique acoustic modes are generated in

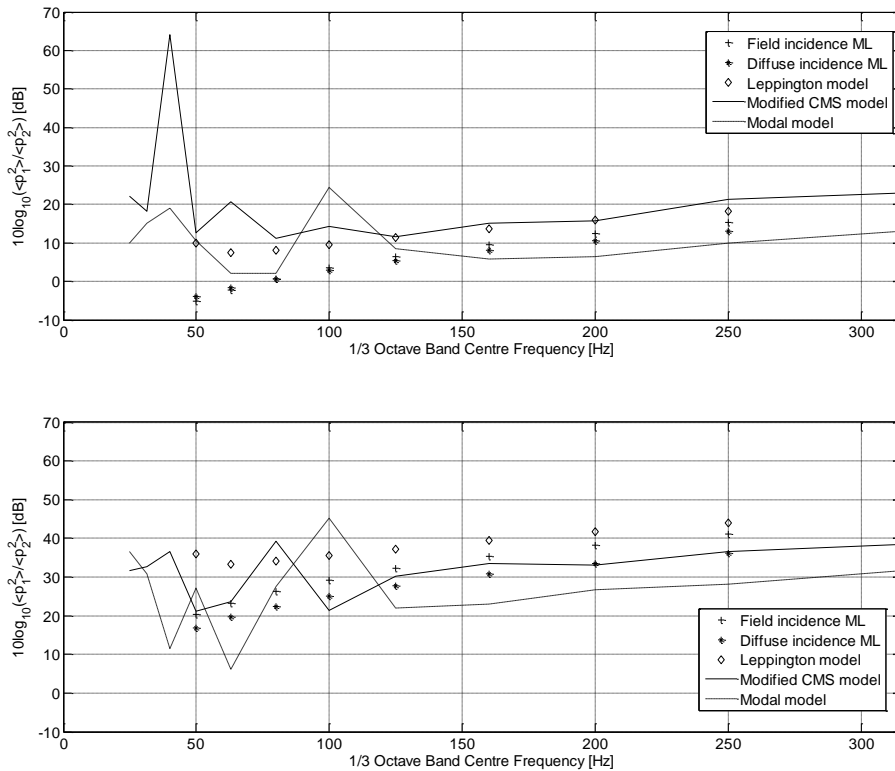


Figure 3: The variation of the Noise Reduction ( $NR = 10 \log_{10} (\langle \bar{p}_1^2 \rangle / \langle \bar{p}_2^2 \rangle)$ ) [dB re 1] in 1/3 octave bands normalized to the system power input. (a). The panel mass per unit area is equal to  $\rho h = 8.06 \text{ kg/m}^2$  and  $E = 2.12 \times 10^9 \text{ N/m}^2$ . (b) The panel mass per unit area is equal to  $\rho h = 78.50 \text{ kg/m}^2$  and  $E = 210 \times 10^9 \text{ N/m}^2$ . The subscript 1 and 2 indicates source and receiving volumes respectively; — CMS model; - - - Modal model; \*\*\* Diffuse incidence Mass Law; +++ Field incidence Mass Law; ◇◇◇ Leppington's prediction.

the receiving room.

#### 4.2 Comparison between the modified 3D and the 1D CMS models

A second example is presented herein in order to compare the 3D CMS model presented herein and the 1D CMS model developed previously [Magalhaes and Ferguson (2003)].

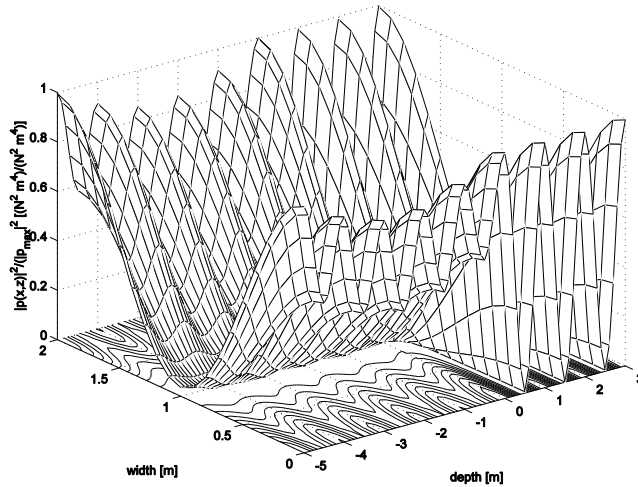
A flexible partition with dimensions and density equal to  $2\text{m} \times 2\text{m}$  and  $806 \text{ kg/m}^3$  respectively was considered over the whole common interface. The thickness,

Young's modulus and Poisson's ratio for the partition were  $0.01\text{m}$ ,  $2.12 \times 10^{-9} \text{N/m}^2$ , and  $0.24$  respectively. Its fundamental natural frequency is  $3.8 \text{ Hz}$ . The source and receiving room dimensions were as before equal to  $5\text{m} \times 2\text{m} \times 2\text{m}$  and  $3\text{m} \times 2\text{m} \times 2\text{m}$  respectively. A constant volume velocity source was placed at one corner of the source room  $(-5,0,0)$ . As mentioned above, the following results are presented in terms of the mean square pressure and particle velocity distribution at  $190 \text{ Hz}$ . The mean square values are normalized to their maximum value in the plane. The normal particle velocity values presented in this section were considered in the  $x$  direction normal to the partition. The mean square pressure and particle velocity distributions were symmetric with respect to the principal axes of both rooms.

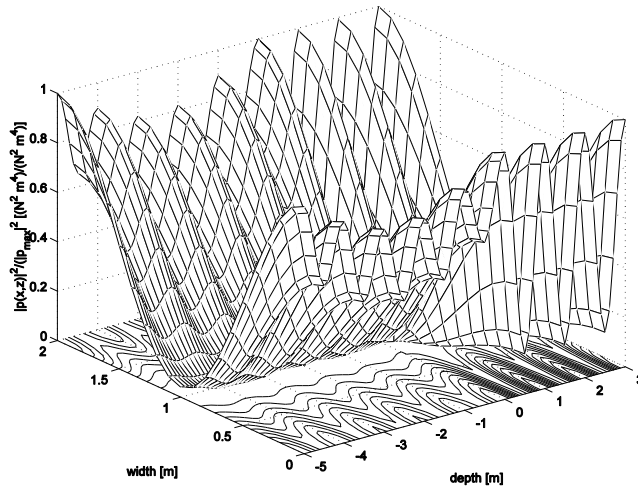
Fig. 4 presents the normalized mean square pressure distribution with respect to the vertical plane  $x-z$  along the centre line length of the room ( $y = 1 \text{ m}$ ) at  $190 \text{ Hz}$ . The pressure at the end wall  $x = -5\text{m}$ , where the source was located, assumed a maximum value. It can be seen that good agreement was found between the modal and CMS model for the mean square pressure distribution. Similarly there is good agreement for the mean square particle velocity distribution (not shown). The results are close to particular modes of both rooms. For instance the natural frequency at  $190.1 \text{ Hz}$  corresponds to the modes  $(5,0,1)$  and  $(3,0,1)$  for the source and receiving rooms respectively. Nevertheless, in terms of mean square pressure distribution the results obtained via the Modal and CMS models present some differences for the receiving room.

The sound pressure value in the source and receiving rooms tended to zero at frequencies below their first 'elastic' modes, i.e. at  $34 \text{ Hz}$  and  $56.7 \text{ Hz}$  as the 'zero order' mode has not been considered in this example. Peaks at  $34 \text{ Hz}$  and  $68 \text{ Hz}$  can be seen in both the source and receiving rooms. However, there are some 'extra' peaks in the receiving room which correspond to the coupled modes of the system. For example, the peak at about  $19 \text{ Hz}$  corresponds to the coupled mode  $19.3 \text{ Hz}$  shown in Table 2.

In Fig 5 a comparison is made between the one dimensional CMS model, which considers a limp partition and was presented previously [Magalhaes and Ferguson (2003)], and the actual modified three-dimensional CMS model in terms of average mean square sound pressure. Figs. 5a and 5b show the results for the source and receiving room respectively. It is seen that the resonance peaks for the CMS-1D model tend to match those for the CMS-3D model as frequency increases. According to the Figs., the first resonance peak for the 1D case is lower than the one for the 3D case, which considers an 'elastic' partition. This is due to the effect of the partition elastic properties, which is considered in the modified 3D CMS model. Some agreement can be seen near the 1D modes as expected.

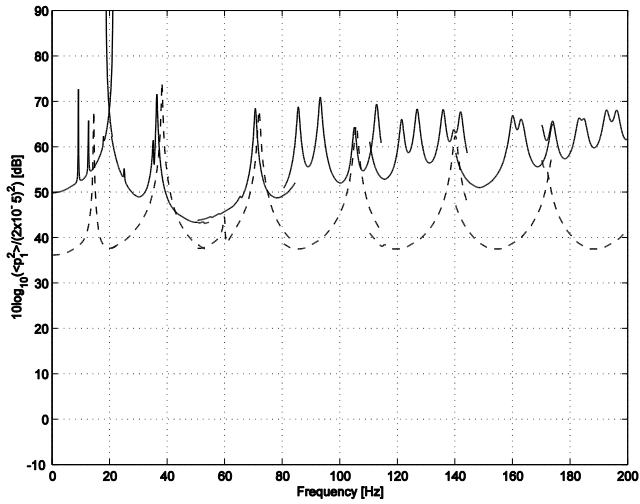


(a)

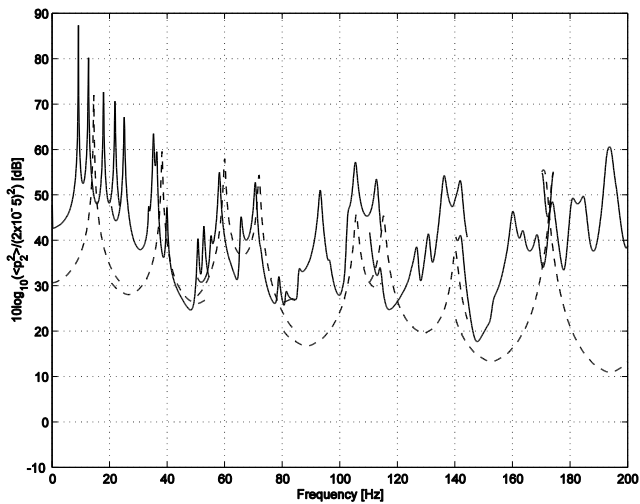


(b)

Figure 4: Normalized mean square pressure distribution with respect to the horizontal plane  $y = 1\text{ m}$  at  $190\text{ Hz}$ . The square elastic partition has dimensions, mass per unit area and Young's Modulus equal to  $2\text{ m} \times 2\text{ m}$ ,  $\rho h = 8.06\text{ kg/m}^2$  and  $E = 2.12 \times 10^9\text{ N/m}^2$  respectively. (a) CMS model and (b) Modal model in relative pressure levels to the maximum in the plane.



(a)



(b)

Figure 5: Comparison between the CMS-1D and the CMS-3D models in terms of the variation of spatial-average mean square sound pressure with frequency (0.1 Hz resolution). The square elastic partition has dimensions, mass per unit area and Young's Modulus equal to  $2\text{m} \times 2\text{m}$ ,  $\rho h = 8.06 \text{ kg/m}^2$  and  $E = 2.12 \times 10^9 \text{ N/m}^2$  respectively. (a)  $10 \log_{10} (\langle \bar{p}_1^2 \rangle / p_o^2)$  [dB re  $2 \times 10^{-5} \text{ Pa}$ ]; (b)  $10 \log_{10} (\langle \bar{p}_2^2 \rangle / p_o^2)$  [dB re  $2 \times 10^{-5} \text{ Pa}$ ]. The subscript 1 and 2 indicates source and receiving rooms respectively; — CMS-3D model; - - - CMS-1D model.

Table 2: The first nine undamped ‘eigenvalues’ of rooms and partition for the CMS Model considering a flexible partition with dimensions  $2\text{m} \times 2\text{m}$ . Mass per unit area and Young’s Modulus are  $\rho h = 8.06 \text{ kg/m}^2$  and  $E = 2.12 \times 10^9 \text{ N/m}^2$  respectively. ‘ $f_1$ ’ and ‘ $f_2$ ’ are the ‘eigenvalues’ corresponding to the fixed-fixed normal modes for the source and receiving rooms. ‘F’ is the coupled frequency with subscripts 1, 2 and ‘p’ representing the source room, receiving room and partition respectively. The subscripts c,3D and c,1D represent the 3D and 1D CMS models respectively. N.B. Note degenerate modes for the coupled models because of symmetry in the square cross-section of the panel and volumes.

$f_1(\text{Hz})$	$f_2(\text{Hz})$	$f_p(\text{Hz})$	$F_{c,3D}(\text{Hz})$	$F_{c,1D}(\text{Hz})$
34.0	56.7	3.8	8.1	12.8
68.0	85.0	9.5	11.2	36.2
85.0	85.0	9.5	11.2	58.9
85.0	102.2	15.2	15.8	69.5
91.5	102.2	18.9	19.3	102.8
91.5	113.3	18.9	19.3	114.7
102.0	120.2	24.6	24.5	136.7
108.9	132.9	24.6	24.5	170.0
108.9	141.7	32.2	34.6	171.4
			34.6	
			37.8	

## 5 Conclusions

The study presented herein is an alternative for improving the quality, reliability and reproducibility of the results. Firstly, it is verified that the CMS technique is a reliable approach which provides a rapid and practical analysis of fluid-structure interaction.

Secondly, the modified 3D CMS approach outlined in this study should be a cost-effective technique that can be used in place of traditional CMS techniques which depend on the use of costly equipments due to the computational efforts. The CMS approach for the three-dimensional problem [Magalhaes and Ferguson (2005)] has been optimized in this paper and the structural component was removed from the analytical formulation by including the structural modes as the constraint modes in the acoustic components. Thus, the performance of the modified 3D CMS model has approximately improved ten percent (10%) in terms of the total computer running time.

Thirdly, the modified CMS model developed herein has been a more effective model in comparison with the modal model. The application described the coupling of two similar rectangular volumes separated by an elastic partition which might form only partial coverage of a common interface with all of the rest being rigid. For the present examples considered it has been possible to use existing analytical expressions for the modes under certain assumptions, e.g. simply-supported edges for the partition, and then rapid numerical calculations for the coupled systems have been possible. The modal model, which considers rigid-walled modes, is more representative at higher frequencies where the system boundary conditions are much less important.

Next, important findings from the simulations performed are when comparison is made between this modified 3D CMS and the 1D CMS model [Magalhaes and Ferguson (2003)]. As mentioned previously the 1D model is not appropriated for real room acoustics problems as tangential and oblique modes are dominant on the modal acoustic response.

Finally, the number of modes, and hence the order of the equations, increases significantly and for practical computational and numerical reasons this modified CMS approach is only useful for low frequency predictions. This comment is also applicable to the existing modal methods and is a consequence of the high modal density with increasing frequency for acoustic volumes and is a reason why statistical approaches (e.g. SEA) have been developed.

**Acknowledgement:** The author gratefully acknowledges the financial support provided by the Minas Gerais State Research Foundation (FAPEMIG). Thanks also go to the Federal University of Minas Gerais (UFMG), University of Southampton (UK) and Dr. Mauro L. C. Magalhaes.

## References

- Craig Jr., R. R.** (1981): *Structural Dynamics – An Introduction to Computer Methods*. John Wiley & Sons, New York.
- Desmet, W.; Van Hal, B.; Sas, P.; Vandepitte D.** (2002): A Computationally Efficient Prediction Technique for the Steady-State Dynamic Analysis of Coupled Vibro-Acoustic Systems. *Advances in Engineering Software*; vol. 53, pp. 527–540.
- Fahy, F. J.** (2000): *Foundation of Engineering Acoustics*. Academic Press London.
- Fahy, F. J.** (1985): *Sound and Vibration*. Academic Press London.
- Ghlaim, K. H.; Martin, K. F.** (1986): Reduced Component Modes in a Damped System. *Proc. Int. Conf. On Modal Analysis, Schenectady*, N. Y. Union College, pp. 683-689.

**Gialamas, T. P.; Tsahalis, D. T.; Otte, D.; Van Der Auwaraer, H.; Manolas, D. A.** (2001): Substructuring Technique: Improvement by Means of Singular Value Decomposition (SVD). *Journal of Applied Mechanics*, vol. 62, pp. 1211-1219.

**Gravvanis, G. A.; Fidelis-Papadopoulos, C. K.; Matiskanidis, P. I.** (2014): Algebraic Multigrid Methods Based on Generic Approximate Banded Inverse Matrix Techniques. *CMES: Computer Modeling in Engineering & Sciences*, vol. 100, pp. 263-281.

**Klein, L. R.; Dowell, E. H.** (1974): Analysis of Modal Damping by Component Modes Method Using Lagrange Multipliers. *Journal of Applied Mechanics*, pp. 527-528.

**Leppington, F. G.; Broadbent, E. G.; Heron, K. H.** (1989): The Transmission of Randomly Incident Sound Through an Elastic Panel. *CMES: Proceedings of the Royal Society of London. Series A, Math. and Physical Sciences*, A426, pp. 153-165.

**Magalhaes, M. D. C; Ferguson, N. S.** (2001): Low frequency airborne sound transmission. *Proceedings of the Internoise*, pp. 1111-1114.

**Magalhaes, M. D. C; Ferguson, N. S.** (2003): Acoustic-Structural Interaction Analysis Using the Component Mode Synthesis Method. *Applied Acoustics*. vol. 64, pp. 1049-1067.

**Magalhaes, M. D. C; Ferguson, N. S.** (2005): The development of a Component Mode Synthesis (CMS) model for three dimensional fluid-structure interaction. *J. Acoust. Soc. Am.*, vol. 118, pp. 3679-3691.

**Magalhaes, M. D. C.** (2012): Sound Power Variation Sensitivity and Variability Using a hybrid Numerical Model. *CMES: Computer Modeling in Engineering & Sciences*, vol. 89, pp. 263-281.

**Meirovitch, L.** (1967): Analytical Methods in Vibrations. *Macmillan*, New York.

**Pierce, A. D.** (1981): Acoustics: An Introduction to its Physical Principles and Applications. *McGraw-Hill New York*.

**Pluymer, B.; Desmet, W.; Vandepitte, D.; Sas, P.** (2002): Application of the wave based prediction technique for the analysis of the coupled vibro-acoustic behaviour of a 3D cavity. *Proc. of ISMA - International Conference on Noise and Vibration Engineering*. KUL, Belgium, pp. 891-900.

**Razzaq, M.; Tsotskas, C.; Kipouros, T.; Savill, M.; Hron, J.** (2013): Multi-Objective Optimization of a Fluid Structure Interaction Benchmarking. *CMES: Computer Modeling in Engineering & Sciences*, vol. 90, no. 4, pp. 313-337.

**Santos, S. R.; Matioli, L. C.; Beck A. T.** (2012): New Optimization Algorithms for Structural Reliability Analysis. *CMES: Computer Modeling in Engineering &*

*Sciences*, vol. 83, no. 1, pp. 23-56.